Medium-polarization effects in $^3SD_1$ spin-triplet pairing

Wenmei Guo,[1,2] U. Lombardo,[1,*] and P. Schuck[3,4]
[1]*Laboratori Nazionali del Sud (INFN), Via S. Sofia 62, 95123 Catania, Italy*
[2]*Institute of Theoretical Physics, Shanxi University, 030006 Taiyuan, China*
[3]*Institut de Physique Nucléaire, Université Paris-Sud, F-91406 Orsay Cedex, France*
[4]*LPMMC (UMR5493), Université Grenoble Alpes and CNRS, 25, Rue des Martyrs, B.P. 166, 38042 Grenoble, France*

(Received 22 August 2018; published 11 January 2019)

Stimulated by the still puzzling competition between spin-singlet and spin-triplet pairing in nuclei, the $^3SD_1$ neutron-proton pairing is investigated in the framework of BCS theory of nuclear matter. The medium-polarization effects are included in the single-particle spectrum and also in the pairing interaction starting from the G matrix, calculated in the Brueckner-Hartree-Fock approximation. The vertex corrections due to spin and isospin collective excitations of the medium are determined from the Bethe-Salpeter equation in the random-phase approximation (RPA) limit, taking into account the tensor correlations. It is found that the self-energy corrections confine the superfluid state to very low density, while remarkably quenching the magnitude of the energy gap, whereas the induced interaction has an attractive effect. The interplay between spin-singlet and spin-triplet pairing is discussed in nuclear matter as well as in finite nuclei.

DOI: 10.1103/PhysRevC.99.014310

I. INTRODUCTION

For several decades the strong experimental evidence of spin-singlet pairing between like nucleons in nuclei has been stimulating intense theoretical activity [1]. In contrast, there is not yet clear evidence for neutron-proton (np) spin-triplet pairing. This is the reason why this kind of pairing has received much less attention [2–4]. However, it has been well known for a long time that the isospin $T = 0$ np interaction could give a relevant pairing, being more attractive than the $T = 1$ interaction [5]. In recent calculations on the competition between spin-singlet and spin-triplet pairings in $N = Z$ nuclei it has been argued that the latter is hindered by the spin-orbit splitting [6–8]. However, in Ref. [6] it is pointed out that in very large $N = Z$ nuclei ($A > 140$) spin-triplet pairing condensates are favored because the spin-orbit force becomes vanishing small. The disappearance of the $S = 1$, $T = 0$ pairing with asymmetry in nuclei has been studied in, e.g., Ref. [9]. In those calculations no dynamical effects on pair correlations are considered, whereas it is proved that particle-vibration coupling could yield a significant contribution to the pairing gap magnitude in the spin-singlet case [10] and also in the neutron-proton spin triplet one, even if less significant [11].

Studies of neutron-neutron (nn) and proton-proton (pp) pairing in nuclear matter have also addressed the medium collective excitations [12,13], which can enhance or quench the pairing correlations according to the nuclear environment where the Cooper pairs are embedded. In the case spin-singlet nn pairing in symmetric nuclear matter the medium-induced interaction significantly enhances the gap, supporting calculations of energy gaps in $^1S_0$ nn or pp spin-singlet pairing in nuclei, where pair vibrations are included [10].

In the case of spin-triplet np pairing BCS calculations with bare interaction in nuclear matter predict sizable energy gaps of the order of 12 MeV, i.e., four times that of the spin singlet [14]. Even if significant rescaling is expected from the self-energy effects, the energy gap could be still large enough by antiscreening due to the induced interaction [12]. Therefore the predicted effect of the spin-orbit energy splitting could be resized by the large spin-triplet pair correlation energy.

In this paper we discuss the $^3SD_1$ spin-triplet np pairing in symmetric nuclear matter, taking into account both self-energy insertions to the quasiparticle spectrum and vertex corrections to the bare interaction due to collective excitations of the medium. The vertex corrections have been determined from the random-phase approximation (RPA) version of the Bethe-Salpeter (BS) equation in the Landau limit. However the RPA does not consider the feedback of the effective interaction on the collective modes which have generated it.

As driving term, the Brueckner-Hartree-Fock (BHF) G matrix is adopted to prevent divergences due to the hard core of the nuclear force. The strong tensor force present in the bare interaction deeply affects the G matrix so that it cannot be neglected. This entails that the tensor parameters must be included in the effective interaction, the solution of the BS equation, when expressed in terms of Landau-Migdal parameters [15]. The resulting energy gap will be compared with the $^1S_0$ spin-singlet nn (or pp) gap, and estimates based on the local density approximation (LDA) will be made for the gaps in nuclei.

*Corresponding author: lombardo@lns.infn.it; At Laboratori Nazionali del Sud (INFN), Via S. Sofia 62, 95123 Catania, Italy.

II. THEORETICAL FRAMEWORK

A. Gap equation

In this section, the formalism of the BCS theory of the $^3SD_1$ superfluid state of symmetric nuclear matter is set, including the medium-polarization effects [14]. The two coupled gap equations ($L = 0, 2$) are written as

$$\Delta_L^{ST}(k) = -\frac{Z_F^2}{\pi}\int_0^\infty k'^2 dk' \sum_{L'} \frac{V_{LL'}^{ST}(k,k')}{\sqrt{\varepsilon_k^2 + \Delta(k')^2}}\Delta_{L'}^{ST}(k'), \tag{1}$$

where

$$\Delta(k)^2 = \Delta_0^{ST}(k)^2 + \Delta_2^{ST}(k)^2. \tag{2}$$

The prefactor Z_F (or Z factor) is the quasiparticle strength, which takes into account the depletion of the Fermi surface [16]. The quasiparticle spectrum is given by

$$E_k^2 = (\varepsilon_k - \varepsilon_F)^2 + \Delta(k)^2, \tag{3}$$

where $\varepsilon_k = k^2/2m^* + U_0$ is the single-particle energy in the effective mass approximation (EMA) and ε_F is the Fermi energy. In a consistent approach the the gap equation has to be coupled to the conservation of the particle number:

$$\rho = 4\sum_k \frac{1}{2}\left[1 - \frac{\varepsilon_k - \varepsilon_F}{E_k}\right], \tag{4}$$

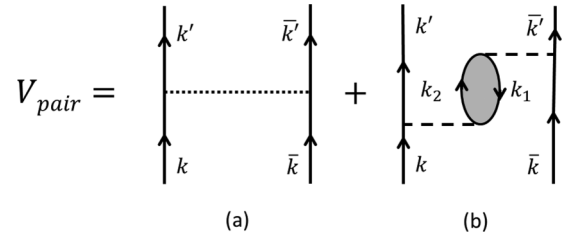

FIG. 1. Pairing interaction with screening: the first term on the right-hand side is the bare interaction; the second one is the induced interaction, where the dashed bubble insertion is the series of ring diagrams.

The pairing force, in principle, contains all irreducible interaction diagrams, but here only the NN bare interaction and the medium-polarization insertions will be considered, as displayed in Fig. 1. The bare two-particle interaction is

$$V^{jst}(\boldsymbol{k},\boldsymbol{k}') = N_0^{-1}\sum Y_{lm}^*(\hat{k})Y_{l'm'}(\hat{k}')C(lm, ss_z|jj_z) \times C(l'm', ss_z'|jj_z)V_{ll'}^{jst}(k,k'), \tag{5}$$

where j, s, and t are total angular momentum, spin, and isospin.

B. Induced interaction in RPA

In this section, we discuss the derivation p-h effective interaction $\mathscr{F}_{SM,SM'}^T(k,k';p)$ leading to the vertex corrections in the pairing interaction, Eq. (13). It fulfills the BS equation in the RPA limit [17]:

$$\mathscr{F}_{SM,SM'}^T(k,k';p) = G_{SM,SM'}^T(k,k';p) + \sum_{M''}\int \frac{d^4k''}{(2\pi)^4} G_{SM,SM''}^T(k,k'';p)\lambda(k'',p)\mathscr{F}_{SM'',SM'}^T(k'',k';p), \tag{6}$$

where the k, k', and q stand for energy-momentum and energy-momentum transfer, respectively, and S and T are total p-h spin (with z projection M) and isospin, respectively. $\lambda(k,q)$ is the free polarization propagator [18]. The solution of the BS equation assumes an algebraic form and can be solved analytically [19] in the Landau limit, where energy and momentum lie on the Fermi surface and energy-momentum transfer $q = 0$. In that limit the driving term $G(\boldsymbol{k},\boldsymbol{k}';0)$ depends only on the angle θ between $\boldsymbol{k}$ and $\boldsymbol{k}'$ and, expressed in terms of Landau parameters (expanded in partial waves), can be written

$$G(\boldsymbol{k},\boldsymbol{k}') = N_0^{-1}\sum_l \left(F_l + F_l'\boldsymbol{\tau}_1\cdot\boldsymbol{\tau}_2 + G_l\boldsymbol{\sigma}_1\cdot\boldsymbol{\sigma}_2 + G_l'\boldsymbol{\sigma}_1\cdot\boldsymbol{\sigma}_2\boldsymbol{\tau}_1\cdot\boldsymbol{\tau}_2 + \frac{q^2}{k_F^2}H_l S_{12}(q) + \frac{q^2}{k_F^2}H_l' S_{12}(q)\boldsymbol{\tau}_1\cdot\boldsymbol{\tau}_2\right)P_l(\cos\theta), \tag{7}$$

where $2\boldsymbol{q} = \boldsymbol{k} - \boldsymbol{k}'$ is the relative momentum and S_{12} the tensor operator, $S_{12}(q) = 3(\vec{S}\cdot\hat{q})^2 - S^2$. $P_l(\cos\theta)$ are the Legendre polynomials. The inclusion of the tensor Landau parameters is motivated by the fact that the interaction contains a strong tensor component in the $^3SD_1$ channel.

In the BS equation the choice of the driving term plays a crucial role. In principle it contains all irreducible processes of the interaction. The simplest approximation is to take the bare interaction itself, but, to prevent the divergences related to the hard core of the nuclear force, we adopted the Brueckner G matrix calculated in the Brueckner-Hartree-Fock (BHF) approximation. The relation between the G matrix and the Landau parameters is presented in Appendix.

In order to derive the BS equation in the Landau limit, we follow closely Ref. [19]. After expanding in partial waves the p-h interaction $\mathscr{F}$ (the same for the driving term),

$$\mathscr{F}_{SM_S,SM_S'}^T(\boldsymbol{k},\boldsymbol{k}';0) = N_0^{-1}\sum_{\substack{lml'm'\\JM}} \frac{4\pi Y_{lm}^*(\hat{k})Y_{l'm'}(\hat{k}')}{[(2l+1)(2l'+1)]^{1/2}}\langle lm\ SM_S|JM\rangle\langle l'm'\ SM_S'|JM\rangle\mathscr{F}_{ll'}^{SJT}, \tag{8}$$

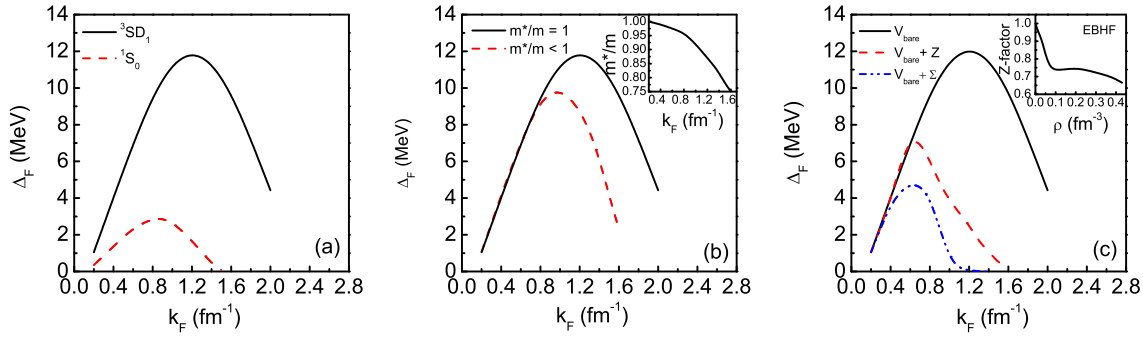

FIG. 2. Energy gap with self-energy effects. Left: Comparison between $^3SD_1$ and $^1S_0$ gaps from bare interaction. Middle: $^3SD_1$ gaps with single-particle spectrum in the EMA (effective mass vs density in the inset). Right: Energy gap with depleted Fermi surface (Z factor vs density in the inset).

the BS equation becomes the algebraic equation for the $\mathscr{F}_{ll'}^{SJT}$ matrix elements,

$$\mathscr{F}_{ll'}^{SJT} = G_{ll'}^{SJT} - \sum_{l''} \frac{1}{2l''+1} G_{ll''}^{SJT} \mathscr{F}_{l''l'}^{SJT}, \tag{9}$$

where J is the total angular momentum. The matrix elements $G_{ll''}^{SJT}$ are the coefficients of the partial-wave expansion of the driving term. Their expression in terms of the Landau parameters is reported in the Appendix. In the case of $S = 0$ all partial-wave matrix elements are diagonal, because the tensor force does not affect the scalar Landau parameters and we simply get the well known expression

$$\mathscr{F}_{ll}^{0JT} = \frac{G_{ll}^{0JT}}{1 + G_{ll}^{0JT}/(2l+1)}, \tag{10}$$

where $G_{ll}^{0J0} = F_l$ and $G_{ll}^{0J1} = F'_l$ and $J = l$.

In the case of $S = 1$, off-diagonal matrix elements also exist due to the coupling between vector and tensor Landau parameters as shown in the Appendix. But only two different angular momenta $(l, l+2)$ at most can couple together. The explicit expression of the matrix elements $\mathscr{F}_{ll}^{0JT}$ $(l' \neq l)$ of the effective interaction is

$$\begin{aligned} \mathscr{F}_{ll}^{1JT} &= D^{-1}\left[G_{ll}^{1JT}\left(1 + \frac{G_{l'l'}^{1JT}}{2l'+1}\right) - \frac{\left(G_{ll'}^{1JT}\right)^2}{2l'+1}\right], \\ \mathscr{F}_{ll'}^{1JT} &= D^{-1} G_{ll'}^{1JT}, \end{aligned} \tag{11}$$

where

$$D = \left(1 + \frac{G_{ll}^{1JT}}{2l+1}\right)\left(1 + \frac{G_{l'l'}^{1JT}}{2l'+1}\right) - \frac{\left(G_{ll'}^{1JT}\right)^2}{(2l+1)(2l'+1)}. \tag{12}$$

Notice that only two different angular momenta at most can couple together, i.e., $l = l'$ or $|l - l'| = 2$.

C. Induced interaction in the p-p sector

For application to the gap equation, the p-h interaction must be converted into p-p interaction and then the induced part must be taken out (second diagram on the right-hand side of Fig. 1). The spin-isospin transformation is given by

$$\begin{aligned} &\mathscr{F}_{pp}^{st}(\boldsymbol{q}, \boldsymbol{P}) \\ &= (-)^{1+t} \sum_{ST} (2T+1) \begin{Bmatrix} \frac{1}{2} & \frac{1}{2} & T \\ \frac{1}{2} & \frac{1}{2} & t \end{Bmatrix} \\ &\quad \times \sum_{MM'mm'} \{SM, SM'|sm, sm'\} \mathscr{F}_{SM_S, SM'_S}^{T}(\boldsymbol{k}, \boldsymbol{k}'; 0), \end{aligned} \tag{13}$$

where $\{SM, SM'|sm, sm'\}$ is the spin transformation bracket and $\boldsymbol{P}$ is the total momentum [20]. For application to the np pairing interaction in the $^3SD_1$ the $\mathscr{F}_{ll'}^{01}$ partial waves with $l, l' = 0, 2$ have to be projected out from the expansion of $\mathscr{F}^{st}(\boldsymbol{q}, \boldsymbol{P})$.

III. NUMERICAL RESULTS

The numerical evaluation of the medium-polarization effects starts from the G matrix calculated in the BHF approximation with the Argonne AV18 two-body interaction and the consistent meson-exchange three body force [21].

From the G-matrix expansion of the self-energy the dispersion effects of the mean-field are included in the effective mass approximation (EMA), and the depletion of the Fermi surface is also approximated by the Z factors [22].

The medium polarization is described by the BS equation, solved in the RPA, where the G^{ph} matrix is the input, so that p-p short-range correlations and p-h long-range collective excitations of the nuclear matter are simultaneously treated in a unified context.

Finally the p-p interaction induced by the medium polarization is added to the bare interaction and the gap equation is solved.

A. Self-energy corrections

As shown in Fig. 2(a), the energy gap with only bare interaction gives for the spin-triplet $^3SD_1$ pairing a peak value the order of 12 MeV, which should be compared with the value of 3 MeV for spin-singlet $^1S_0$ pairing [14]. The large difference between the two gaps is justified by the exponential dependence on the interaction strength of the solution of the BCS

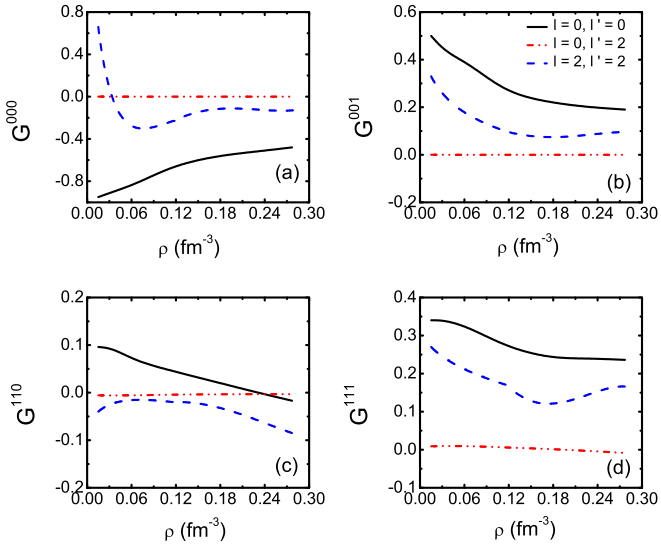

FIG. 3. Driving p-h interaction $\mathscr{G}_{ll'}^{SJT}$ from the G matrix in the SD channel.

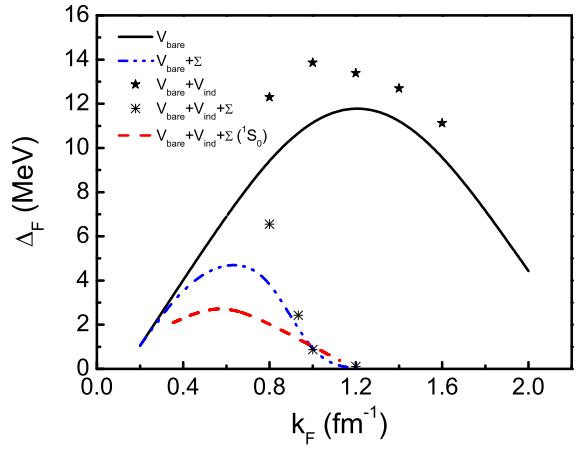

FIG. 4. Comparison among $^3SD_1$ gaps from RPA induced interaction and previous effects and $^1S_0$ in full calculations.

gap equation [18]. In Fig. 2(b) the mean-field dispersive effect is also reported for comparison using the effective mass (see inset) in the quasi-particle spectrum, according to Eq. (3). This effect is well known [23]: the gap magnitude gets reduced and pairing density range is also shifted towards low densities, where $m^*/m \approx 1$. Additional reduction of the gap is obtained when including the depletion of the Fermi sphere, as shown in Fig. 2(c). The depletion is introduced via the Z factor [16,22], plotted in the inset of the figure. This quenching effect is more pronounced since pairing strength is exponentially dependent on Z^2. The two combined effects give rise to a remarkable quenching of the gap in a density range, making the $^3SD_1$ pairing a surface effect like the $^1S_0$ one. However, the peak value of the $^3SD_1$ energy gap is still over two times larger than the $^1S_0$ one with the same self-energy approximation.

B. Induced interaction

The p-p matrix elements of the G matrix in the SD channel are calculated from the BHF approximation with the same two- and three-body forces as the self-energy. The p-p matrix elements are transformed into p-h matrix elements, expressed in terms of Landau parameters as shown in the Appendix. For such a purpose the Landau limit has been adopted, where the energy-momentum transfer is assumed to be vanishing. Since the SD components of the G matrix derive from the tensor part of the bare interaction, the additional H and H' Landau parameters have been introduced in the particle-hole (p-h) effective interaction [24]. In Fig. 3 the SD partial waves of the BHF Landau parameters are plotted as a function of the density; see Eqs. (A5)–(A9) for $T = 0$ and the corresponding ones for $T = 1$. The zero-order diagonal components are the Landau parameters from the BHF G matrix with no tensor force effect. The $S = 1$ partial-wave components are affected by the tensor Landau parameters, but their effect is small. It follows that the off-diagonal matrix elements are even smaller. The main contribution comes from the isoscalar and isovector density fluctuations ($S = 0$) as expected. From the solution of the BS equation in the Landau limit with BHF Landau parameters shown in Fig. 3 as input, the effective interaction is determined and transformed in the particle-particle (p-p) representation, according to Eq. (13). The matrix elements of the $^3SD_1$ induced part (second diagram of the right-hand side of Fig. 4) are reported in Table I. It easily seen that the dominant contribution is concentrated in the $S = 0$ isoscalar matrix element. This contribution is attractive, much the same as for the spin-singlet pairing in symmetric nuclear matter [12].

C. Pairing gap from vertex corrections

The p-p effective interaction is added to the pairing interaction and the BCS equation is solved. The resulting gap vs Fermi momentum is displayed in Fig. 4 in comparison with the preceding results. Two series of calculations have been performed: the first one (upper stars) shows the effects on induced interaction without self-energy corrections; the second one (lowest stars) consists of full calculations: self-energy plus induced interaction. There was a limit to the lower densities imposed by the missing convergence of the BHF calculation of the G matrix. This is due to the singularity of the G matrix in the density domain where large pair correlations

TABLE I. p-p induced interaction $(\mathscr{F}_{pp}^{10})_{ll'}$ in the $^3SD_1$ channel.

ρ (fm^{-3})	k_F (fm^{-1})	SS (MeV fm^3)	DD (MeV fm^3)	SD (MeV fm^3)
0.277	1.60	−0.70	−0.03	0.04
0.228	1.50	−1.14	−0.04	0.02
0.186	1.40	−1.63	−0.04	0.00
0.175	1.36	−1.65	0.05	−0.01
0.117	1.20	−3.43	−0.05	−0.04
0.068	1.00	−13.03	−0.07	−0.08
0.035	0.80	−22.32	0.00	−0.10
0.015	0.60	−28.40	0.09	−0.10

TABLE II. Average gaps Δ_0 (no screening) and Δ (screening) in $N = Z$ nuclei from LDA. The density profiles are taken from Ref. [26].

A	R (fm)	Δ_0 (MeV)	Δ (MeV)
40	3.83	6.82	3.54
100	5.20	8.18	3.75
200	6.50	9.38	4.00

are expected to occur. This drawback requires a self-consistent calculation of the BCS equation and a BHF calculation with the quasiparticle energy spectrum, that is beyond the scope of the present investigation. The main result is that, due to the attractive nature of the new term, the self-energy quenching is reduced, but less than in the case of spin-singlet pairing. A second main result is that the shift of the peak value at low density produced by the self-energy is not affected by the induced interaction, suggesting that pairing is a surface phenomenon in finite nuclei. Finally, it is worth noticing that the spin-triplet pairing in the $^3SD_1$ channel is still much larger than the spin-singlet pairing in the $^1S_0$ channel, as clearly shown in Fig. 4.

D. Average pairing in nuclei from LDA

To make contact with pairing in nuclei we have estimated the average gap in $N = Z$ nuclei from the Thomas-Fermi density corresponding to the states around the chemical potential μ defined as follows [25]:

$$\langle\Delta(\mu)\rangle = \int d\vec{r} \sum_i \frac{1}{g(\mu)}\delta(\mu - \varepsilon_i)|\phi_i(\vec{r})|^2\Delta(r), \quad (14)$$

where $\phi_i(\vec{r})$ is the single-particle wave function with energy eigenvalue ε_i, $\Delta(r)$ is the nuclear matter gap for the density $\rho(r)$ according to the local density approximation (LDA), and $g(\mu)$ is the level density at μ. It easy to show that, in the $\hbar \Rightarrow 0$ semiclassical limit [25],

$$\langle\Delta(\mu)\rangle = \frac{\int d^3\vec{r}\,\Delta(r)\rho^{1/3}(\vec{r})}{\int d^3\vec{r}\,\rho^{1/3}(\vec{r})}, \quad (15)$$

where we take for the density the phenomenological one parametrized by [26]. In Table II the results are reported for some $N = Z$ nuclei. We see that screening substantially reduces the gap values which, however, remain stronger than in the $T = 1$ channel.

IV. DISCUSSION AND CONCLUSIONS

In this paper the spin-triplet $^3SD_1$ pairing in symmetric nuclear matter has been discussed within the BCS theory with medium-polarization effects. On one hand, the self-energy corrections reduce significantly the gap magnitude, shifting the peak value to low density. On the other hand, the induced interaction, which is attractive almost in the full asymmetry range, partially restores a higher magnitude of the gap without squeezing the density range of the superfluid phase. The induced interaction has been obtained in the RPA in the Landau limit starting from the BHF p-h interaction. In this way the long-range correlations are built up on top of the short-range correlations included in the G matrix. In this approximation the main contribution comes from the scalar density fluctuations, as expected. On the other hand the feedback of the vertex correction on the other spin-isospin fluctuations can be treated only in the framework of the induced interaction approach [27], which is a task of further investigations.

However, the gaps obtained in the present approximation, as large as 2–3 times the magnitude of the spin-singlet pairing in the $^1S_0$ channel, provide a strong indication of the importance of the medium polarization. The conclusion is that the $^3SD_1$ neutron-proton superfluid state in nuclear matter turns out to be more stable than the $^1S_0$ neutron-neutron or proton-proton superfluid state. This is in agreement with recent calculations, where it is found that, in $N = Z$ nuclei with mass higher than $A = 140$, np pair correlations are stronger than nn or pp ones [6]. Under such a threshold the pairing between like nucleons is found to be the favored one, because the spin-orbit splitting in nuclei hinders np pairing. Nevertheless the present nuclear matter calculations do not exclude the possibility that the np pairing strength is much larger in the spin triplet than the singlet even below $A = 140$. It would be a timely issue to study the competition between spin-triplet pairing and the spin-orbit force in finite nuclei including medium screening effects.

ACKNOWLEDGMENTS

The authors are grateful to G. L. Colo' and E. Vigezzi for useful discussions. This work was supported by the INFN post-doctorate fellowship program and the National Natural Science Foundation of China under Grant No. 11705109.

APPENDIX

The microscopic derivation of the Landau parameters from the BHF approximation is obtained by converting the p-p G matrix, as calculated with the Brueckner-Bethe-Goldstone equation, into the p-h representation. This procedure yields [28,29]

$$(F, F') = \frac{1}{16}\sum_{st}(2t \pm 1)G^{st}, \quad (A1)$$

$$(G, G') = \frac{1}{16}\sum_{t}(2t \pm 1)(G^{1t} - G^{0t}), \quad (A2)$$

$$(H, H') = \frac{1}{24}\frac{k_F^2}{q^2}\sum_{t}(2t \pm 1)\left(\tilde{G}_1^{1t} - \tilde{G}_0^{1t}\right), \quad (A3)$$

where G^{st} denotes the G matrix with spin s and isospin t, and $\tilde{G}_m^{st}$ is the same with $\hat{q}$ along the spin quantization axis. The isoscalar (isovector) Landau parameters take the upper (lower) sign. Inverting the partial-wave expansion of the driving term,

we can determine the coefficients

$$G_{ll'}^{SJT} = N_0 \frac{[(2l+1)(2l'+1)]^{1/2}}{4\pi} \sum_{m,m',M_S,M_S'} [(2l+1)(2l'+1)]^{1/2} \langle lm\, SM_S | JM\rangle \langle l'm'\, SM_S' | JM\rangle$$
$$\times \int d\hat{k}\, d\hat{k}' Y_{lm}(\hat{k}) Y_{l'm'}^*(\hat{k}') \langle SM_S, T | G^{ST}(\boldsymbol{k}, \boldsymbol{k}') | SM_S', T\rangle, \tag{A4}$$

as a function of the Landau parameters. For $S = 0$ component the calculation is straightforward, whereas for $S = 1$ it is quite tedious for the coupling between vector and tensor Landau parameters. It can be found in the literature (see, e.g., Refs. [17,30]). Below are the matrix elements needed for the calculation of vertex correction to the np pairing interaction in the channel $^3SD_1$. For $T = 0$ they are, in order,

$$G_{00}^{000} = F_0, \tag{A5}$$
$$G_{22}^{020} = F_2, \tag{A6}$$
$$G_{00}^{110} = G_0, \tag{A7}$$
$$G_{22}^{110} = G_2 - \frac{1}{4}\left(\frac{7}{3}H_1 - 2H_2 + \frac{3}{7}H_3\right), \tag{A8}$$
$$G_{02}^{110} = -\frac{\sqrt{10}}{12}\left(3H_0 - 2H_1 + \frac{3}{5}H_2\right). \tag{A9}$$

For $T = 1$ the isoscalar Landau parameters must be replaced by the corresponding isovector ones ($F \to F', \ldots$).

[1] *Fifty Years of Nuclear BCS: Pairing in Finite Systems*, edited by R. Broglia and V. Zelevinsky (World Scientific, Singapore, 2013).
[2] W. Satula and R. Wyss, Phys. Lett. B **393**, 1 (1997).
[3] A. Poves and G. Martinez-Pinedo, Phys. Lett. B **430**, 203 (1998).
[4] A. L. Goodman, Phys. Rev. C **60**, 014311 (1999).
[5] A. M. Lane, *Recent Developments in Nuclear Theory, Frontiers in Physics* (Benjamin, New York, Amsterdam, 1964).
[6] G. F. Bertsch and Y. Luo, Phys. Rev. C **81**, 064320 (2010).
[7] G. F. Bertsch, in *Fifty Years of Nuclear BCS*, edited by R. A. Broglia and V. Zelevinsky (World Scientific, Singapore, 2012).
[8] H. Sagawa, C. L. Bai, and G. Colo, Phys. Scr. **91**, 083011 (2016).
[9] T. Sogo, G. Röpke, and P. Schuck, Phys. Rev. C **82**, 034322 (2010).
[10] F. Barranco, P. F. Bortignon, R. A. Broglia, G. Colo, and E. Vigezzi, Eur. Phys. J. A **11**, 385 (2001); F. Barranco, P. F. Bortignon, R. A. Broglia, G. Colo, P. Schuck, E. Vigezzi, and X. Vinas, Phys. Rev. C **72**, 054314 (2005).
[11] E. Litvinova, C. Robin, and I. A. Egorova, Phys. Lett. B **776**, 72 (2018).
[12] L. G. Cao, U. Lombardo, and P. Schuck, Phys. Rev. C **74**, 064301 (2006).
[13] S. S. Zhang, L. G. Cao, U. Lombardo, and P. Schuck, Phys. Rev. C **93**, 044329 (2016).
[14] U. Lombardo, in *Nuclear Methods and Nuclear Eqution of State*, edited by M. Baldo, Int. Rev. of Nucl. Phys. Vol. 8 (World Scientific, Singapore, 1999), pp. 458–510.
[15] A. B. Migdal, *Theory of Finite Fermi Systems and Applications to Atomic Nuclei* (Interscience, London, 1967).
[16] W. Dickhoff and D. van Neck, *Many Body Theory Exposed!* (World Scientific, Singapore, 2008).
[17] W. H. Dickhoff, A. Faessler, H. Müther, and S. S. Wu, Nucl. Phys. A **405**, 534 (1983).
[18] A. L. Fetter and J. D. Walecka, *Quantum Theory of Many Particle Systems* (McGraw-Hill, New York, 1971).
[19] B. L. Friman and A. K. Dhar, Phys. Lett. B **85**, 1 (1979).
[20] W. H. Dickhoff, A. Faessler, J. Meyer-ter-Vehn, and H. Müther, Phys. Rev. C **23**, 1154 (1981).
[21] P. Grange, A. Lejeune, M. Martzolff, and J. F. Mathiot, Phys. Rev. C **40**, 1040 (1989); A. Lejeune, U. Lombardo, and W. Zuo, Phys. Lett. B **477**, 45 (2000).
[22] J. M. Dong, U. Lombardo, and W. Zuo, Phys. Rev. C **87**, 062801 (2013).
[23] M. Baldo, J. Cugnon, A. Lejeune, and U. Lombardo, Nucl. Phys. A **515**, 409 (1990); **536**, 349 (1991).
[24] S. O. Bäckman, O. Sjöberg, and A. D. Jackson, Nucl. Phys. A **321**, 10 (1979).
[25] P. Ring and P. Schuck, *The Nuclear Many-Body Problem* (Springer, Berlin, 2000).
[26] S. Shlomo, Nucl. Phys. A **539**, 17 (1992).
[27] S. V. Babu and G. E. Brown, Ann. Phys. **78**, 1 (1973).
[28] S.-O. Bäckman, Nucl. Phys. A **120**, 593 (1968).
[29] J. Dabrowski and P. Haensel, Can. J. Phys. **52**, 1768 (1974).
[30] K. Nakayama, S. Krewald, J. Speth, and W. G. Love, Nucl. Phys. A **431**, 419 (1984).